Eur. J. Mineral.
2018, **30**, 1173–1180
Published online 3 September 2018

Gabrielsonite revisited: crystal-structure determination and redefinition of chemical formula

Natale PERCHIAZZI[1,*], Ulf HÅLENIUS[2], Pietro VIGNOLA[3] and Nicola DEMITRI[4]

[1]Dipartimento Di Scienze Della Terra, Universita' di Pisa, via Santa Maria 53, 56126 Pisa, Italy
*Corresponding author, e-mail: natale.perchiazzi@unipi.it
[2]Department of Geosciences, Swedish Museum of Natural History, PO Box 50007, 10405 Stockholm, Sweden
[3]CNR-Istituto per la dinamica dei processi ambientali, via Botticelli 23, 20131 Milano, Italy
[4]Elettra – Sincrotrone Trieste S.C.p.A., S.S. 14 km 163, 5 in area science park – loc. Basovizza, 34149 Trieste, Italy

Abstract: A reinvestigation of gabrielsonite from the holotype specimen from Långban, central Sweden, using single-crystal synchrotron X-ray diffraction, electron-microprobe techniques and Fourier-transform infrared (FTIR) spectroscopy, Raman and Mössbauer spectroscopies show that the mineral is an anhydrous Fe^{3+}-bearing arsenite and not a hydrous Fe^{2+}-bearing arsenate, as originally proposed. The revised ideal chemical formula of gabrielsonite is $PbFe^{3+}(As^{3+}O_3)O$. The mineral is related to the descloizite supergroup, but it differs through the valencies of the non-Pb cations Fe (M^{3+} *vs.* M^{2+}) and As (3 + *vs.* 4 +) and through lower coordination of Pb (4 *vs.* 7–8) and As (3 *vs.* 4). The redefinition of gabrielsonite (proposal 17-G) has been approved by the Commission on New Minerals, Nomenclature and Classification (CNMNC) of the International Mineralogical Association.

Key-words: gabrielsonite; Långban; lead iron arsenite; Mössbauer; FTIR; Raman spectroscopy; crystal structure; synchrotron single-crystal study; mineral formula redefinition.

1. Introduction

The worldwide famous mineral locality Långban is one of a group of related mines clustered within ~20 km of each other near the S-E border of the Swedish province of Värmland, in the Palaeoproterozoic Bergslagen ore province. Stratabound Fe–Mn oxide ores, enriched in Pb, As, Sb and Ba, occur in a metamorphosed felsic metavolcanic suite together with carbonate rocks and skarns (Magnusson, 1930; Moore, 1970; Nysten *et al.*, 1999). Nearly 300 mineral species are known for the locality, of which some 30 are found here only. Especially lead arsenites, arsenates and oxychlorides are among the rarest minerals: as detailed in Table 1, Långban is the type locality for four lead arsenates, eight lead arsenites and two lead oxychlorides. These exotic lead minerals, especially oxychlorides, are typically found also as secondary phases in ancient smelting slags at, *e.g.*, Baratti, Italy (Franzini & Perchiazzi, 1992; Pasero *et al.*, 1997) and Lavrion, Greece (Gelaude *et al.*, 1996). Presently it is estimated that approximately 570 different mineral species are known in Lavrion slags, formed by the interaction between sea-water and slags hosting heavy metals such as Pb, Cu, As. The richness of the Lavrion mineral parageneses is demonstrated by the recent discovery of two new lead chloride arsenites, described by Siidra *et al.* (2011, 2012).

Gabrielsonite was defined as a new species by Moore (1967), who reported a full description of the physical properties, chemical composition and crystallography of the new phase. Gabrielsonite was discovered on specimens collected at Långban (Hindenburg stope) and stored in the mineralogical collections of the Naturhistoriska Riksmuseet, Stockholm. Weissenberg single-crystal study allowed him to define the mineral as orthorhombic $P2_1ma$, with cell parameters a = 7.86(1) Å, b = 5.98(1) Å, c = 8.62(1) Å, Z = 4 and D_{calc} = 6.69 g cm^{-3}, D_{meas} = 6.67 g cm^{-1}. Preliminary qualitative spectrographic and EPMA analyses showed the presence of major Pb, Fe, As with minor Sb, Bi, Si, Mn and traces of Na, Ca. Quantitative chemical data were obtained through wet chemical analysis (Table 2), pointing to the crystal-chemical formula $(Pb_{0.90}Fe_{0.07})_{\sum 0.97}Fe_{0.97}(AsO_4)(OH_{0.55}O_{0.12})_{\sum 0.67}$. On the basis of chemical and crystallographic data, Moore (1967) assigned gabrielsonite to the descloizite–pyrobelonite group of minerals.

The present study of gabrielsonite started within the frame of the SYNTHESYS funded visit SE-TAF-5983 to Naturhistoriska Riksmuseet, Stockholm. Material for the study was selected from the holotype specimen, preserved in the mineralogical collections with registration number #19250353.

2. Experimental procedure

2.1. Mössbauer spectroscopy

A room-temperature ^{57}Fe Mössbauer spectrum (Fig. 1) was collected in transmission mode using a conventional constant acceleration spectrometer with a nominal 50 mCi

https://doi.org/10.1127/ejm/2018/0030-2794 0935-1221/18/0030-2794 $ 3.60

Table 1. Lead arsenates, arsenites and oxychlorides first discovered at Långban. (1) Lundström, 1874; (2) Breithaupt, 1830; (3) Chukanov *et al.*, 2011; this study; (4) Aminoff, 1934; (5) Nordenskiöld, 1877; (6) Dunn & Rouse, 1985; (7) Aminoff, 1923; (8) Moore, 1967; (9) this study; (10) Flink, 1888; (11) Dunn *et al.*, 1979; (12) Dunn *et al.*, 1986; (13) Flink, 1920; (14) Gabrielson *et al.*, 1958; (15) Gillberg, 1960.

	Arsenates
Caryinite[(1)]	$(Na, Pb)(Ca, Na)CaMn_2^{2+}(AsO_4)_3$
Hedyphane[(2)]	$Ca_2Pb_3(AsO_4)_3Cl$
Långbanshyttanite[(3)]	$Pb_2Mn_2Mg(AsO_4)_2(OH)_4{\cdot}6H_2O$
Sahlinite[(4)]	$Pb_{14}(AsO_4)_2O_9Cl_4$
	Arsenites
Ecdemite[(5)]	$Pb_6Cl_4(As_2O_7)$
Freedite[(6)]	$Cu^+Pb_8(AsO_3)_2O_3Cl_5$
Finnemanite[(7)]	$Pb_5(AsO_3)_3Cl$
Gabrielsonite[(8, 9)]	$PbFe^{3+}(As_3{+}O_3)O$
Heliophyllite[(10)]	$Pb_6Cl_4(As_2O_7)$
Paulmooreite[(11)]	$Pb_2[As_2O_5]$
Rouseite[(12)]	$Pb_2Mn^{2+}[AsO_3]_2{\cdot}2H_2O$
Trigonite[(13)]	$Pb_3Mn^{2+}(AsO_3)_2(HAsO_3)$
	Oxychlorides
Blixite[(14)]	$Pb_2(O,OH)_2Cl$
Perite[(15)]	$PbBiClO_2$

Table 2. Chemical data (wt%) for gabrielsonite: (a) Moore (1967); (b) calculated values for the ideal $PbFe^{3+}(As^{3+}O_3)O$ end-member formula; (c) and (d) this study: mean and range.

	(a)	(b)	(c)	(d)
Fe_2O_3	0.0	19.86	20.23	19.63–20.63
PbO	50.09	55.53	53.84	52.28–55.97
CaO			0.01	0.00–0.04
MnO			0.12	0.02–0.19
FeO	18.47		0.4	
As_2O_3		24.61	24.95	23.83–25.82
Sb_2O_3			0.13	0.00–0.23
V_2O_3			0.02	0.00–0.04
As_2O_5	28.54			
H_2O	1.21			
Total	98.31	100.00	99.7	

^{57}Co source in Rh matrix. The sample absorber was prepared by pressing finely ground powder of gabrielsonite with a powdered acrylic resin to a self-supporting disc with a 1.25 cm diameter. The mineral powder was prepared from hand-picked gabrielsonite crystal fragments and was checked for purity by powder X-ray diffraction (pXRD). The amount of powder used was 11 mg resulting in an absorber with a Fe-thickness of ~1.3 mg/cm^2. Spectral data for the velocity range ±4.2 mm/s were recorded in a multichannel analyzer using 512 channels. Results were calibrated against a high-purity α-Fe foil (25 µm thick) and the raw data were folded to 256 channels. The spectrum was fitted assuming Lorentzian peak shapes using the MossA fitting program (Prescher *et al.*, 2012), with the results presented in Table 3.

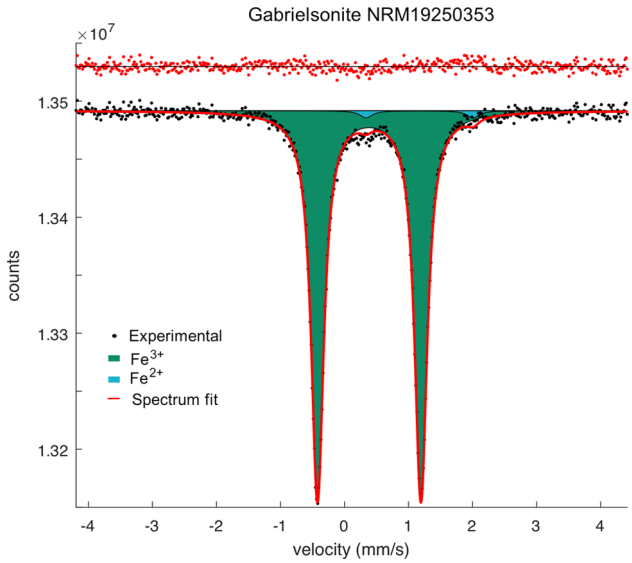

Fig. 1. Room-temperature ^{57}Fe Mössbauer spectrum of gabrielsonite (online version in colour).

Table 3. Hyperfine parameters for quadrupole doublets in the Mössbauer spectrum of gabrielsonite.

	CS (mm/s)	QS (mm/s)	FWHM (mm/s)	Intensity (%)
Fe^{3+}	0.386 (1)	1.615 (2)	0.241 (2)	98.3 (7)
Fe^{2+}	1.173 (43)	1.671 (85)	0.232 (132)	1.7 (7)

2.2. Micro-Raman spectroscopy

The unpolarized micro-Raman spectrum for gabrielsonite (Fig. 2) was obtained on a polished sample employed for electron-probe microanalysis (EPMA), working in backscattered geometry with a Jobin-Yvon Horiba XploRA Plus apparatus, equipped with a motorized *x-y* stage and an Olympus BX41 microscope with a 100×/0.75 objective lens. The Raman spectra were excited by the 532 nm emission of a solid-state laser attenuated to 25% intensity, and the system was calibrated using the 520.5 cm^{-1} Raman band of Si before every experimental session. Spectra were collected through repeated multiple acquisitions with single counting times of 30 s, and backscattered radiation were analyzed with a 1200 mm^{-1} grating monochromator.

2.3. Fourier-transform infrared spectroscopy

Polarized Fourier-transform infrared spectroscopy (FTIR) absorption spectra (Fig. 3) in the wavenumber range 500–5000 cm^{-1} were measured at a resolution of 2 cm^{-1} on a 38 µm thick, cut and polished section of a gabrielsonite single crystal using a Bruker Vertex spectrometer equipped with a Hyperion II microscope, a glow-bar source, a KBr beam-splitter, a LN_2-cooled MCT detector and a ZnSe polarizer. In addition, an unpolarised FTIR spectrum was recorded with the same instrument on a powdered gabrielsonite sample in a pressed KBr-disc.

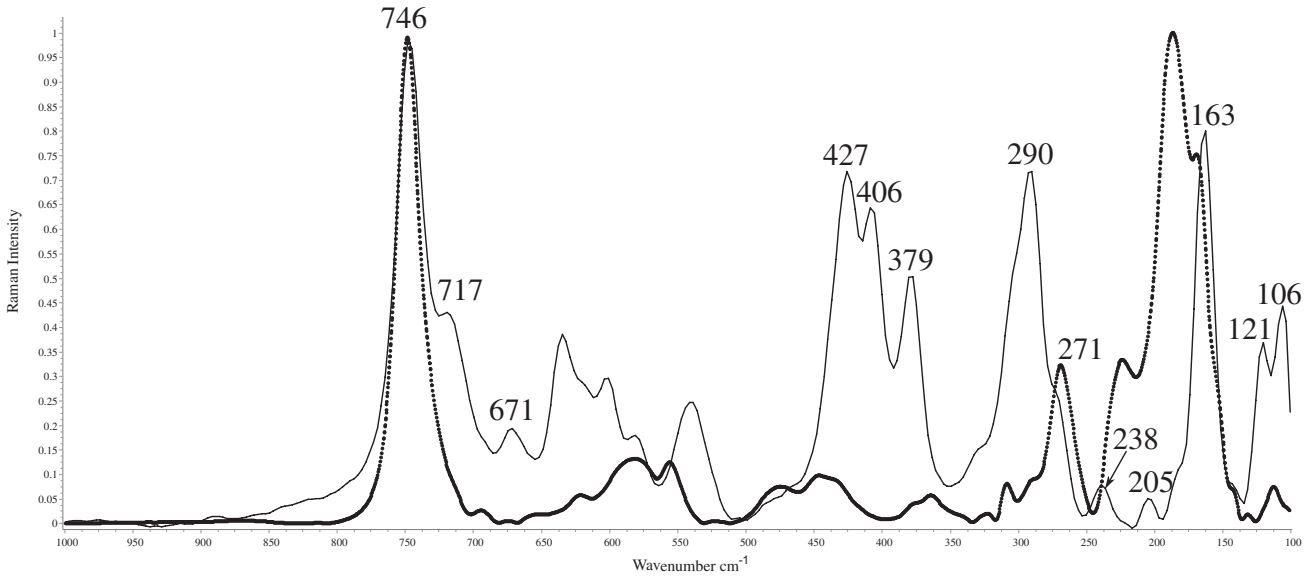

Fig. 2. Raman spectrum of gabrielsonite (solid line) compared with spectrum of trigonite (dotted thick line).

2.4. EPMA chemical study

Quantitative chemical analyses (Table 2) were performed on a polished and carbon-coated section of a gabrielsonite fragment, for a total of 10 analysis points, using a JEOL JXA-8200 electron microprobe working in wavelength-dispersion mode, at the laboratory of the Department of Earth Sciences "A. Desio", University of Milan (ESD-MI). The system was operated using an accelerating voltage of 15 kV, a beam current of 5 nA, a spot size of 7 µm, and a counting time for one spot analysis of 30 s on peak and 10 s on the right and left backgrounds. The following substances were used as standards: graftonite KF-16 (Fransolet, 1975) for P, Fe, Mn and Ca; realgar for As; olivine for Mg; hornblende for F; scapolite for Cl; pure metals (99.99 wt%) for Sb and V; synthetic PbO for Pb. Following the Mössbauer spectroscopy and the structural analysis indications, all the iron and arsenic are reported as trivalent. Phosporus, F and Cl were below detection limit in all analyzed points. The raw data were corrected for matrix effects using the $\varphi\rho Z$ method from the JEOL series of programs.

2.5. Single-crystal structural study

Single-crystal intensity data collected at the XRD1 beamline, ELETTRA synchrotron facility, confirmed that the mineral is orthorhombic, a = 7.909(1) Å, b = 6.006(1) Å, c = 8.661(1) Å, with space group $P2_1ma$. The gabrielsonite structure was solved by direct methods with SHELXS-2013 software (Sheldrick, 2013), within the WinGX program suite (Farrugia, 2012). Data pertaining to crystal-structure solution are presented in Table 4.

2.6. Rietveld study

To ascertain the phase homogeneity of the studied sample, a synchrotron X-ray powder diffraction data collection was performed at the XRD1 beamline of ELETTRA synchrotron facility. A 0.5 mm borosilicate capillary was filled with gabrielsonite powder, obtained by grinding in acetone. A Rietveld refinement was performed through the TOPAS-Academic program (Coelho, 2012). The gabrielsonite structure model resulting from the single-crystal study was assumed. Neither cell parameters nor the atomic positional and displacement parameters were subsequently refined. A preliminary Pawley refinement (Pawley, 1981) was performed to get starting values for background, modelled with a function, effective to describe background intensity at low angles due to air scattering, and with a 10-terms Chebyshev

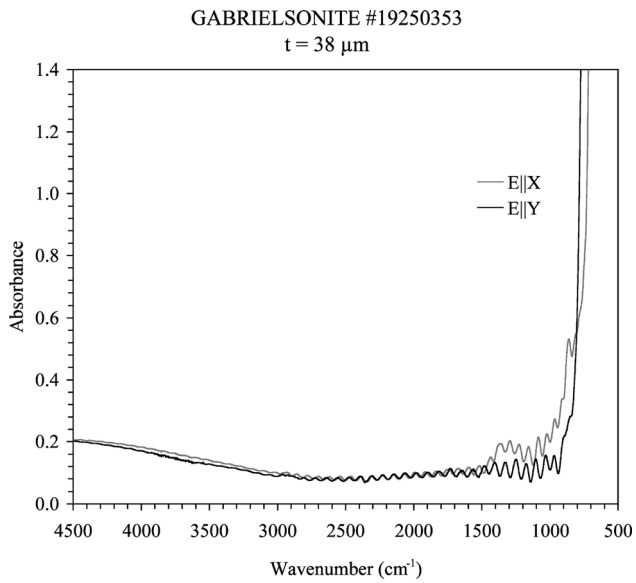

Fig. 3. Polarised single-crystal FTIR-spectra (**E**||X and **E**||Y) of gabrielsonite. A regular low-amplitude pattern visible below ~3200 cm^{-1} is due to interference effects resulting from perfectly polished parallel surfaces of the thin absorber.

Table 4. Experimental details for gabrielsonite single-crystal structural study.

Crystal data	Data collection and refinement
Crystal-chemical formula	Maximum 2θ, 66°
$PbFe^{3+}As^{3+}O_3O$	Synchrotron radiation; λ = 0.5904 Å
Crystal size (mm) 0.12 × 0.10 × 0.08	Collected reflections 8390
Space group $P2_1ma$	Unique reflections 2490, R_{int} = 0.0796
a = 7.909(1) Å	Observed reflections 2380 > 4σ(F_o)
b = 6.006(1)	$-13 \leq h \leq 13$, $-10 \leq k \leq 11$, $-14 \leq l \leq 14$
c = 8.661(1)	$R[F^2 > 4\sigma(F^2)]$, w$R(F^2)$, S 0.039, 0.1140, 1.042
V = 444.41(14) Å^3, Z = 4	No. of parameters, restraints 76, 0
ρ_{calc} = 6.5 g cm^{-3}, ρ_{meas} = 6.67 g cm^{-3}	Flack index 0.024(18)
M = 3.21 cm^{-1}	$\Delta\rho_{max}$, $\Delta\rho_{min}$ (e Å^{-3}) +4.43, −4.61

Table 5. Fractional atomic coordinates and equivalent isotropic displacement parameters (Å^2) for gabrielsonite.

Atom	x	y	z	Mult.	U_{eq}
Pb_1	0.15143(3)	½	0.60333(3)	2	0.01001(2)
Pb_2	0.13986(4)	0	0.89903(3)	2	0.0103(2)
As_1	0.3494(16)	0	0.4416(1)	2	0.0075(3)
As_2	0.8614(2)	½	0.9499(1)	2	0.0072(3)
Fe	0.5334(2)	0.2495(1)	0.74700(7)	4	0.0068(2)
O_1	0.3772(11)	0	0.6495(6)	2	0.0091(9)
O_2	0.6515(11)	½	0.8735(7)	2	0.0086(10)
O_3	0.6433(10)	0	0.8466(6)	2	0.0073(9)
O_4	0.4398(10)	½	0.6272(6)	2	0.0077(9)
O_5	0.8434(9)	0.2747(6)	1.0852(5)	4	0.0120(8)
O_6	0.2028(6)	0.2250(6)	0.4279(5)	4	0.0120(8)

function. The effect of asymmetry and zero error were accounted for, and found negligible. The instrumental contribution to the peak shape was modelled through a pseudo-Voigt function, by fitting the data of a sample of SRM 660a (LaB_6) collected under the same experimental setup. Peak-shape broadening was modelled taking into account Gaussian crystallite size and microstrain contributions. The refinement yielded R_{wp} = 3.903, R_{exp} = 0.707, R_p = 2.943, GoF = 5.521, confirming gabrielsonite as the only phase present in detectable amounts in the analyzed powder.

3. Discussion

The recorded Mössbauer spectrum (Fig. 1) shows a dominant quadrupole doublet with a centre shift (CS) of 0.39 mm/s and a quadrupole splitting (QS) of 1.61 mm/s (Table 3). These hyperfine parameters are typical for ferric iron located in a distorted octahedral coordination (*e.g.*, Coey, 1984). The observed QS-value of 1.61 mm/s suggests that the $Fe^{3+}O_6$-polyhedron in gabrielsonite experience a strong distortion comparable to the one recorded for the $M3O_6$-polyhedron in the epidote structure (*e.g.*, Grodzicki *et al.*, 2001). In addition to the dominant Fe^{3+}-doublet, a very weak quadrupole doublet with hyperfine parameters typical for ferrous iron in 6-coordination (Table 3) is observed in the Mössbauer spectrum of gabrielsonite. The recorded Fe^{3+}/Fe_{tot} ratio is ~0.98.

A limited number of Raman studies of arsenite minerals are present in literature, and not all of these studies report combined chemical and X-ray data, essential for an adequate mineralogical characterization. As an example, Raman data for finnemanite, $Pb_5(AsO_3)_3Cl$ from Flinders Range, Australia, are reported by Bahfenne & Frost (2010), without any other data supporting mineral identification. These data differ substantially from data reported by Bahfenne *et al.* (2011) for finnemanite from Långban, characterized by X-ray diffraction. Raman data for paulmooreite, $Pb_2As_2O_5$, from Långban are reported by Bahfenne *et al.* (2012). Raman data for trigonite, $Pb_3Mn^{2+}(AsO_3)_2(HAsO_3)$, obtained on material from the type locality, characterized by combined Mössbauer, EPMA and X-ray single-crystal studies, are available in RRUFF database (Lafuente *et al.*, 2015). Raman spectra of synthetic orthoarsenites were moreover reported in several studies, *e.g.* Liu *et al.* (2014) and Đorđević (2015).

In Fig. 2 Raman data for gabrielsonite are compared with data for the related mineral trigonite, as reported in RRUFF database. The remarkable similarity of the two Raman spectra fully confirms the chemical nature of gabrielsonite as a lead arsenite. Band assignment for gabrielsonite can be performed on the basis of the sequence of band energies reported by Nakamoto (1997), namely with $\nu_1 > \nu_3 > \nu_2 > \nu_4$.

In the spectral region 500–1000 cm^{-1} gabrielsonite shows strong bands due to the symmetric As–O ν_1 (746 cm^{-1}) and antisymmetric ν_3 (717, 671 cm^{-1}) stretching modes,

Table 6. Selected bond distances (Å) for gabrielsonite.

Pb_1		Pb_2		As_1		As_2		Fe	
$-O_6(\times 2)$	2.280(4)	$-O_3$	2.203(5)	$-O_6(\times 2)$	1.784(5)	$-O_2$	1.786(8)	$-O_3$	1.935(5)
$-O_4$	2.290(8)	$-O_5(\times 2)$	2.309(6)	$-O_1$	1.814(5)	$-O_5(\times 2)$	1.796(4)	$-O_4$	1.972(4)
$-O_4$	2.606(6)	$-O_1$	2.862(7)					$-O_6$	2.028(6)
								$-O_2$	2.083(5)
								$-O_5$	2.096(6)
								$-O_1$	2.118(6)

Table 7. Bond valence balance (*v.u.*) for gabrielsonite. Σ_{an} are the sums of the bond strengths reaching each anion.

	O_1	O_2	O_3	O_4	O_5	O_6
Pb_1				0.618		0.635(×2)
				0.263		
Pb_2	0.131		0.782		0.587(×2)	
Fe	0.379	0.416	0.621	0.562	0.402	0.483
	0.379	0.416	0.621	0.562		
As_1	0.935					1.013(×2)
As_2		1.008			0.982(×2)	
Σ_{an}	1.824	1.840	2.024	2.005	1.971	2.131

followed at lower wavenumbers by ν_2 (379, 406, 427 cm^{-1}) deformation mode, and in the region centered on 300 cm^{-1} by ν_4 (290, 271, 304 cm^{-1}) deformation mode. Lastly lattice modes (106, 121, 163, 205, 238 cm^{-1}) appear in the region below 250 cm^{-1}.

The FTIR spectra (Fig. 3) show clearly the absence of absorption bands in the OH-stretching (~3000–3500 cm^{-1}) and OH-bending (~1600 cm^{-1}) regions. Very strong absorbance recorded below ~800 cm^{-1} is related to vibrations in As-centered polyhedra.

The Mössbauer and FTIR data demonstrate that gabrielsonite is anhydrous and that iron in the structure is predominantly ferric.

From EPMA and Mössbauer data, the crystal-chemical formula calculated on the basis of (As + Sb + V) = 1 *apfu* is $(Pb_{0.951}Mn_{0.007}Fe^{2+}_{0.002}Ca_{0.001})_{?0.961}Fe^{3+}_{1.00}(As_{0.995}Sb_{0.004}V_{0.001}O_3)O_{0.960}$.

Atomic positional and displacement parameters and selected bond lengths for gabrielsonite are reported in Tables 5 and 6. The two independent As^{3+} cations occur in the common trigonal pyramidal coordination, with bond distances clustering near the mean value of 1.782 Å for As–(O, OH) distances reported by Majzlan *et al.* (2014). Each of the two independent Pb cations is linked to four oxygen, resulting in a "open" lopsided coordination, with all the four anions asymmetrically located on one side with respect to Pb^{2+}. Each Pb shows three short bonds (2.20–2.30 Å) and one long bond distance; 2.60 Å for Pb_1–O_4 and 2.86 Å for Pb_2–O_1. The two above described anionic dispositions are clear examples of an active "lone pair" effect of Pb^{2+}, with the $6s^2$ inert electron doublet ideally located at the empty apex of a distorted square pyramidal coordination hosting Pb. Fourfold-coordinated Pb is known in a few lead minerals, among these litharge (Dickinson & Friauf, 1924), but has so far not been reported in other Pb arsenites, neither in the minerals of the descloizite supergroup (Đorđević *et al.*, 2016).

As shown in Table 6, Fe is located in a distorted octahedron with a quadratic elongation index (Robinson *et al.*, 1971) QE = 1.0111, in agreement with the results of Mössbauer spectroscopy. The mean Fe–O bond length value is 2.034 Å, quite close to the expected ideal value (2.045 Å) for $^{VI}Fe^{3+}$–O.

As to the oxygen atoms coordination, a tetrahedral coordination is displayed by O_1 and O_4, whereas O_2, O_3, O_5 and O_6 show a triangular coordination.

A bond-valence balance analysis performed according to Brese & O'Keeffe (1991) is reported in Table 7. The valence sums reaching the anions are all close to 2, confirming the absence of hydroxyl in gabrielsonite.

4. Structure description and relation to the descloizite supergroup

The $Fe^{3+}O_6$ polyhedra form edge-sharing octahedral "columns", running along the *b* axis (Fig. 4). The As_2 and Pb_2 polyhedra form corner-sharing heteropolyhedral "chains", running along the *a* axis (Fig. 4b). The Pb_1 polyhedra form corner-sharing "chains" running along the *c* axis, which link through corner sharing to As1 trigonal pyramids, to form heteropolyhedral sheets parallel to (010) (Fig. 4c).

Heteropolyhedral As_1–Pb_1 sheets regularly alternate along (010) with slabs with thickness 4.5 Å, hosting As_2–Pb_2 chains. The As_2–Pb_2 heteropolyhedral chains connect through the long Pb_2–O_1 (2.86 Å) bond to the heteropolyhedral As_1–Pb_1 sheets to form a three-dimensional framework.

Corner sharing between Fe octahedral "chains" and As_1 and As_2 polyhedra give rise to a three-dimensional framework, with Pb cations located within the empty voids of the framework (Fig. 5a).

According to Pertlik (1978), a similar three-dimensional framework is present in the trigonite structure, made up by corner-sharing Mn and As polyhedra, with Pb coordination polyhedra grasped by corner-sharing to this framework (see Fig. 1 in Pertlik, 1978). Pertlik (1978) emphasizes anyway the anisotropic distribution of bonding within the trigonite framework, stressing the occurrence of strongly bonded (010) layers, made up by corner-sharing As_1, As_2, Mn and Pb polyhedra. These layers are connected along (010) only through long Pb–O bonds (Pb_2–O_7 2.89(6) Å, Pb_3–O_2 3.14(6) Å) and "bridging" corner-sharing As3 polyhedra, explaining the perfect (010) cleavage of trigonite (see Fig. 2 in Pertlik, 1978).

Majzlan *et al.* (2014) proposed for arsenites a structural classification based on the considerations reported in Hawthorne *et al.* (2000); in this classification scheme gabrielsonite can be put within the class "*structures with polymerized Asϕ_3 trigonal pyramids and M$\phi_{4\text{-}6}$ polyhedra*", and the subclass "*infinite frameworks of polyhedra*".

In a reference paper on the descloizite supergroup, Đorđević *et al.* (2016) stress the occurrence of two distinct structural types, namely an adelite group, with space-group symmetry $P2_12_12_1$ and a descloizite group, with space-group symmetry *Pnma.* They tentatively included gabrielsonite in the adelite group. As pointed out by these authors, the structures of this supergroup can be described as "columns" of edge-sharing octahedra, linked through corner sharing with arsenate groups to form a three-dimensional framework, in which cavities are hosting large-radius cations such as Pb in descloizite and Ca in adelite. The structural relationships between gabrielsonite and the descloizite supergroup are shown in Fig. 5, where the crystal structures of gabrielsonite and of arsendescloizite are compared, as seen along the axis with ~6 Å periodicity, common to the two phases.

The common feature between the two crystal structures are the edge-sharing octahedral "columns", hosting cations such as Fe^{3+} in gabrielsonite and Zn^{2+} in arsendescloizite. The differences between gabrielsonite and the phases of the descloizite supergroup arise from different oxidation state and coordination of As cations, as well as from the different coordination of Pb^{2+}, seven-fold in the descloizite group and eight-fold in the adelite group, to be compared with the above described asymmetric four-fold coordination in gabrielsonite.

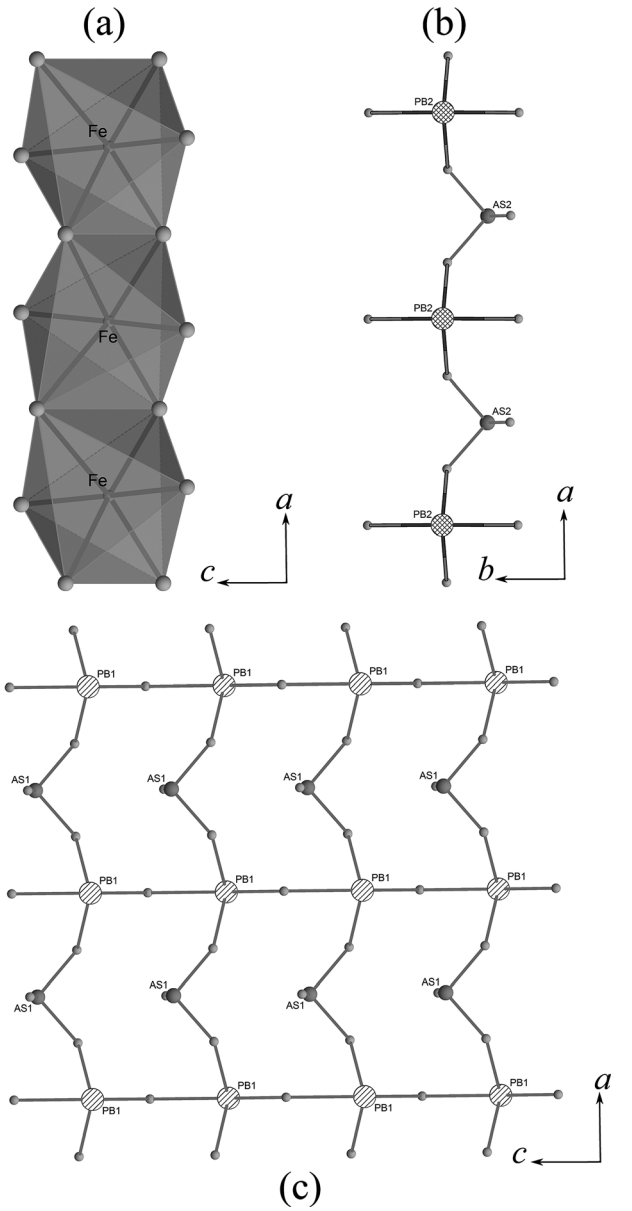

Fig. 4. Polymerisation of coordination polyhedra in gabrielsonite. Fe^{3+} octahedra form edge-sharing "columns" (a) running along *a*. Heteropolyhedral "chains" (b) running along *a* are made up by corner-sharing As_1 and Pb_1 polyhedra, whereas heteropolyhedral "sheets" (c) parallel to (010) are made up by As_2 and Pb_2 polyhedra.

5. Conclusions

A combined crystal-chemical study of gabrielsonite sampled from the holotype specimen confirms the general crystallography proposed by Moore (1967) for the mineral. However, the chemical composition reported by Moore (1967) on the basis of wet chemical analyses is not confirmed. In contrast to the formula $PbFe^{2+}(AsO_4)(OH)$ proposed by Moore (1967), we find on the basis of Mössbauer and FTIR spectroscopic studies that the mineral is anhydrous and that iron occurs almost exclusively in the trivalent state. On the basis of our findings we propose that the ideal formula of gabrielsonite should be revised as $PbFe^{3+}(As^{3+}O_3)O$. The gabrielsonite structure is strongly influenced by the active lone-pair effect displayed by both As^{3+} and Pb^{2+} cations, which consequently adopt an open III and IV coordination, respectively. Notwithstanding a close structural relationship, gabrielsonite do not belong, as hypothesized by Moore (1967) and Đorđević *et al.* (2016), to the descloizite

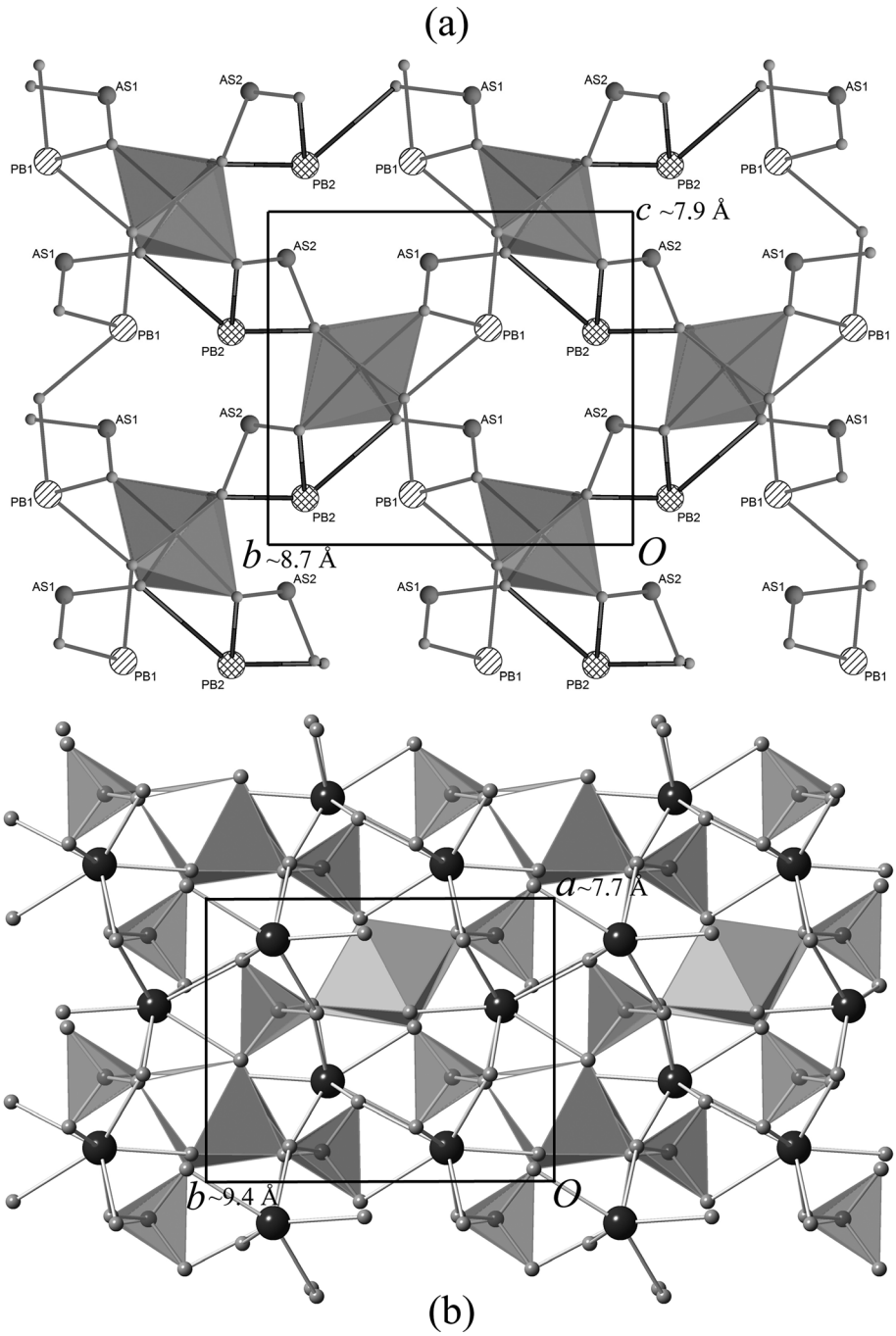

Fig. 5. Comparison of gabrielsonite (a) and arsendescloizite (b) structures, as seen along the axis with ~6 Å periodicity.

supergroup. According to the structural classification proposed by Majzlan *et al.* (2014), gabrielsonite can be placed in the *"structures with polymerized Asϕ_3 trigonal pyramids and M$\phi_{4\text{-}6}$ polyhedra"* class, and in *"infinite frameworks of polyhedra"*.

Acknowledgements: This research received support from the SYNTHESYS Project (http://www.synthesys.info/), which is financed by European Community Research Infrastructure Action under the FP7 "Structuring the European Research Area Programme". This work was financially supported by the University of Pisa through the project PRA_2018_41 "Georisorse e Ambiente". Authors wish to thank A. Pavese, University of Turin, for providing funds for the EPMA analyses.

References

Aminoff, G. (1923): Finnemanit, ett nytt blyarsenit från Långban (Finnemanite, a new lead arsenite from Långban. *Geol. Fören. Stock. För.*, **45**, 160–163.

— (1934): Note on a new mineral from Långban (Sahlinite). *Geol. Fören. Stock. För.*, **56**, 493–494.

Bahfenne, S. & Frost, R.L. (2010): Raman spectroscopic study of the mineral finnemanite $Pb_5(As^{3+}O_3)_3Cl$. *J. Raman Spectr.*, **41**, 329–333.

Bahfenne, S., Rintoul, L., Langhof, J., Frost, R.L. (2011): Single-crystal Raman spectroscopy of natural finnemanite and comparison with its synthesised analogue. *J. Raman Spectr.*, **42**, 2119–2125.

—, —, —, — (2012): Single-crystal Raman spectroscopy of natural paulmooreite $Pb_2As_2O_5$ in comparison with the synthesized analog. *Am. Mineral.*, **97**, 143–149.

Breithaupt, A. (1830): Bestimmung neuer Mineral-Specien, 2. *Hedyphan. J. Chem. Phys.*, **60**, 308–316.

Brese, N.E. & O'Keeffe, M. (1991): Bond-valence parameters for solids. *Acta Crystallogr.*, **B47**, 192–197.

Coelho, A.A. (2012): Topas Academic Version 4.1. Coelho Software, Brisbane.

Coey, J.M.D. (1984): Mössbauer spectroscopy of silicate minerals. *in* "Mössbauer Spectroscopy Applied to Inorganic Chemistry", Long, G.J. ed. Plenum Press, New York and London, 443–509.

Chukanov, N.V., Pekov, I.V., Jonsson, E., Zubkova, N.V., Filinchuk, Y.E., Belakovskiy, D.I., Pushcharovsky, D.Y. (2011): Långban-shyttanite, a new low-temperature arsenate mineral with a novel structure from Långban. Sweden. *Eur. J. Mineral.*, **23**, 675–681.

Dickinson, R.G. & Friauf, J.B. (1924): The crystal structure of tetragonal lead monoxide. *J. Am. Chem. Soc.*, **46**, 2457–2463.

Đorđević, T. (2015): Crystal Chemistry of the $M1^{1+,2+}$–$M2^{2+,3+}$–(H)-arsenites: the first Cadmium (II) Arsenite, $Na_4Cd_7(AsO_3)_6$. *Z. Anorg. Allg. Chem.*, **641**, 1863–1868.

Đorđević, T., Kolitsch, U., Nasdala, L. (2016): A single-crystal X-ray and Raman spectroscopic study of hydrothermally synthesized arsenates and vanadates with the descloizite and adelite structure types. *Am. Mineral.*, **101**, 1135–1149.

Dunn, P.J. & Rouse, R.C. (1985): Freedite and thorikosite from Långban, Sweden, and Laurion, Greece; two new species related to the synthetic bismuth oxyhalides. *Am. Mineral.*, **70**, 845–848.

Dunn, P.J., Peacor, D.R., Sturman, B.D. (1979): Paulmooreite, a new lead arsenite from Långban, Sweden. *Am. Mineral.*, **64**, 352–354.

Dunn, F.J., Peacor, D.R., Sturman, B.D., Wicks, F.J. (1986): Rouseite, a new lead manganese arsenite from Långban. Sweden. *Am. Mineral.*, **71**, 1034–1036.

Farrugia, L.J. (2012): WinGX and ORTEP for Windows: an update. J. Appl. Crystallogr., **45**, 849–854.

— (1888): Heliophyllit von Pajsberg. Öfversigt af Kongliga Vetenskaps-Akademiens Förhandlingar, **45**, 574–578.

Flink, G. (1920): Trigonit och dixenit, två nya mineral från Långbanshytte gruvor. *Geol. Fören. Stock. För.*, **42**, 436–452.

Fransolet, A.M. (1975): Etude minéralogique et pétrologique des phosphates de pegmatites granitiques. Unpublished PhD Thesis, University of Liège, 333 p.

Franzini, M. & Perchiazzi, N. (1992): I minerali delle scorie ferrifere etrusche di Baratti. *Atti Soc. Tosc. Sci. Nat., Mem. Serie A*, **99**, 43–77.

Gabrielson, O., Parwel, A., Wickman, F.E. (1958): Blixite, a new lead-oxyhalide mineral from Långban. *Arkiv Mineral Geol.*, **2**, 411–415.

Gelaude, P., Kalmthout, P., Rewitzer, C. (1996): Lavrion, the minerals in the historic slags. Janssen Print, Nijmegen.

Gillberg, M. (1960): Perite, a new oxyhalide mineral from Långban, Sweden. *Arkiv Mineral. Geol.*, **2**, 565–570.

Grodzicki, M., Heuss-Assbichler, S., Amthauer, G. (2001): Mössbauer investigations and molecular orbital calculations on epidote. *Phys. Chem. Miner.*, **28**, 675–681.

Hawthorne, F.C., Krivovichev, S.V., Burns, P.C. (2000): The crystal chemistry of sulfate minerals. *Rev. Mineral. Geochem.*, **40**, 1–112.

Lafuente, B., Downs, R.T., Yang, H., Stone, N. (2015): Highlights in mineralogical crystallography, W. De Gruyter, Berlin, 1–30.

Liu, J., Jia, R., Liu, J. (2014): The vibration characterization of synthetic crystalline lead hydrogen arsenite chloride precipitates $Pb_2(HAsO_3)Cl_2$, implications of solidification of As (III) and Pb (II). *Spectrochim. Acta Part A*, **117**, 658–661.

Lundström, C.H. (1874): Analyser å tvenne nya svenska mineraler. *Geol. Fören. Stock. För.*, **2**, 178–179.

Magnusson, N.H. (1930): Långbans malmtrakt. Sverigs geologiska undersökning Ca 23, 111 p.

Majzlan, J., Drahota, P., Filippi, M. (2014): Parageneses and crystal chemistry of arsenic minerals. *Rev. Mineral. Geochem.*, **79**, 17–184.

Moore, P.B. (1967): Gabrielsonite, $PbFe(AsO_4)(OH)$, a new member of the descloizite-pyrobelonite group, from Långban. *Arkiv Mineral Geol.*, **4**, 401–405.

— (1970): Mineralogy and chemistry of Långban-type deposits in Bergslagen, *Sweden. Mineral. Rec.*, **1**, 154–172.

Nakamoto, K. (1997): Infrared and raman spectra of inorganic and coordination compounds. Part A: Theory and applications in inorganic chemistry, 5th edn, Wiley-Interscience, New York.

Nordenskiöld, A.E. (1877): Mineralogiska meddelanden 4. Nya mineralier från Långban. *Geol. Fören. Stock. För.*, **3**, 376–384.

Nysten, P., Holtstam, D., Jonsson, E. (1999): The Långban minerals. *in* "Långban, the mines, their minerals, history and explorers", Holtstam, D. & Langhof, J. eds. Raster Förlag, Munich, 215 p.

Pasero, M., Perchiazzi, N., Bigi, S., Franzini, M., Merlino, S. (1997): $Pb_2Fe^{3+}Cl_3(OH)_4{\cdot}H_2O$, a newly discovered natural phase from Tuscany, Italy; physico-chemical data, crystal structure, and OD character. *Eur. J. Mineral.*, **9**, 43–51.

Pawley, G.S. (1981): Unit cell refinement from powder diffraction scans. *J. Appl. Crystallogr.*, **14**, 357–361.

Pertlik, F. (1978): The crystal structure of trigonite, $Pb_3Mn(AsO_3)_2(AsO_2OH)$. *Tschermaks Min. Petrogr. Mitt.*, **25**, 95–105.

Prescher, C., McCammon, C., Dubrowinsky, L. (2012): MossA: a program for analyzing energy-domain Mössbauer spectra from conventional and synchrotron sources. *J. Appl. Crystallogr.*, **45**, 329–331.

Robinson, K., Gibbs, G.V., Ribbe, P.H. (1971): Quadratic elongation – quantitative measure in coordination polyhedra. *Science*, **172**, 567–570.

Sheldrick, G.M. (2013): SHELXS-2013/1, program for the crystal structure solution. University Göttingen, Göttingen, Germany.

Siidra, O.I., Krivovichev, S.V., Chukanov, N.V., Pekov, I.V., Magganas, A., Katerinopoulos, A., Voudouris, P. (2011): The crystal structure of $Pb_5(As^{3+}O_3)Cl_7$ from the historic slags of Lavrion, Greece, a novel Pb(II) chloride arsenite. *Mineral. Mag.*, **75**, 339–348.

Siidra, O.I., Chukanov, N.V., Pekov, I.V., Krivovichev, S.V., Magganas, A., Katerinopoulos, A., Voudouris, P. (2012): $Pb_2(AsO_2OH)Cl_2$, a new phase from the Lavrion ancient slags, Greece: occurrence and characterization. *Mineral. Mag.*, **76**, 597–602.

Received 13 February 2018
Modified version received 30 April 2018
Accepted 30 April 2018